Very-Long-Chain Acyl-Coenzyme A Dehydrogenase Deficiency in Mice

Vernat J. Exil, Richard L. Roberts, Harold Sims, Jacquelin E. McLaughlin, Robert A. Malkin, Carla D. Gardner, Gemin Ni, Jeffrey N. Rottman, Arnold W. Strauss

Abstract—Fatty acid oxidation (FAO) defects are inborn errors of metabolism clinically associated with cardiomyopathy and sudden infant death syndrome (SIDS). FAO disorders often present in infancy with myocardial dysfunction and arrhythmias after exposure to stresses such as fasting, exercise, or intercurrent viral illness. It is uncertain whether the heart, in the absence of stress, is normal. We generated very-long-chain acyl-coenzyme A dehydrogenase (VLCAD)-deficient mice by homologous recombination to define the onset and molecular mechanism of myocardial disease. We found that VLCAD-deficient hearts have microvesicular lipid accumulation, marked mitochondrial proliferation, and demonstrated facilitated induction of polymorphic ventricular tachycardia, without antecedent stress. The expression of acyl-CoA synthase (ACS1), adipophilin, activator protein 2, cytochrome *c*, and the peroxisome proliferator activated receptor γ coactivator-1 were increased immediately after birth, preceding overt histological lipidosis, whereas ACS1 expression was markedly downregulated in the adult heart. We conclude that mice with VLCAD deficiency have altered expression of a variety of genes in the fatty acid metabolic pathway from birth, reflecting metabolic feedback circuits, with progression to ultrastructural and physiological correlates of the associated human disease in the absence of stress. **(*Circ Res*. 2003;93:448-455.)**

Key Words: inborn error of metabolism ■ mitochondrial β-oxidation ■ cardiac lipidosis ■ ventricular arrhythmias ■ sudden infant death syndrome

Mitochondrial fatty acid oxidation is the key metabolic pathway for ATP production in the heart and skeletal muscle. Inborn errors of metabolism affecting this pathway are typically inherited in a recessive fashion. Affected individuals may present with heart and skeletal muscle dysfunction, cardiac arrhythmias, or SIDS (sudden infant death syndrome). Postmortem histological findings almost always include organ lipidosis.[1–8] The observed phenotypes in this illness are induced by physiological stress or by conditions that stimulate fatty acid oxidation, such as starvation or endurance exercise, through mechanisms that are not well understood.

Fatty acids are the preferred substrate for ATP production in the heart after birth. Fatty acids are transported in the blood in the form of lipoprotein or bound to albumin. Long-chain fatty acids are transported through the plasma membranes by fatty acid transporters, such as FATP and CD36/FAT. On entry into the cell, fatty acids are converted to their acyl CoA derivatives by fatty acyl CoA synthase (ACS1). Fuel metabolism requires entry of these acyl moieties into the mitochondrion (using carnitine palmitoyltransferase and acylcarnitine translocase), where they undergo four basic steps known as β-oxidation to produce acetyl CoA and reducing equivalents ($FADH_2$ and NADH). The reducing equivalents subsequently fuel oxidative phosphorylation to produce ATP. The first step of the β-oxidation spiral is an oxidation reaction of acyl CoA that is catalyzed by a family of four homologous enzymes, very-long- (VLCAD C14 to C20), long- (LCAD C10 to C16), medium- (MCAD C6 to C10), and short- (SCAD C4 to C6) chain acyl-CoA dehydrogenases. This reaction forms enoyl CoA and reduces flavin adenine dinucleotide (FAD) to reduced FAD ($FADH_2$).

Disease caused by mutations in the VLCAD gene affects children and young adults, but younger infants present with the most severe form of the disease. Three phenotypes have been described[1]: (1) a severe childhood form with no residual enzyme activity, typically presenting with cardiomyopathy and resulting in high mortality[1,5,7]; (2) a milder childhood form with hypoketotic hypoglycemia as the main feature[1,9]; and (3) an adult presentation with intermittent skeletal myopathy mainly triggered by fasting or exercise.[1]

The biochemical consequences of VLCAD deficiency have been studied in both man[1,5,6,10,11] and mice.[12] However, the

Original received May 6, 2003; revision received July 15, 2003; accepted July 18, 2003.

From the Division of Cardiology, Department of Pediatrics (V.J.E., C.D.G., A.W.S), Department of Pathology (R.L.R.), Division of Cardiovascular Medicine, Department of Internal Medicine and Mouse Metabolic Phenotyping Center (G.N., J.N.R.), Vanderbilt University School of Medicine, Nashville, Tenn; Department of Pediatrics, Division of Pediatric Cardiology (H.S.), Washington University School of Medicine, St Louis, Mo; Joint Program in Biomedical Engineering (J.E.M., R.A.M.); University of Memphis and University of Tennessee Health Sciences Center, Memphis, Tenn.

Correspondence to Dr Vernat Exil, Vanderbilt Children's Hospital, 1161 21st Ave South, D-2220 MCN, Nashville, TN 37232. E-mail vernat.exil@vanderbilt.edu

Circulation Research **is available at http://www.circresaha.org** **DOI: 10.1161/01.RES.0000088786.19197.E4**

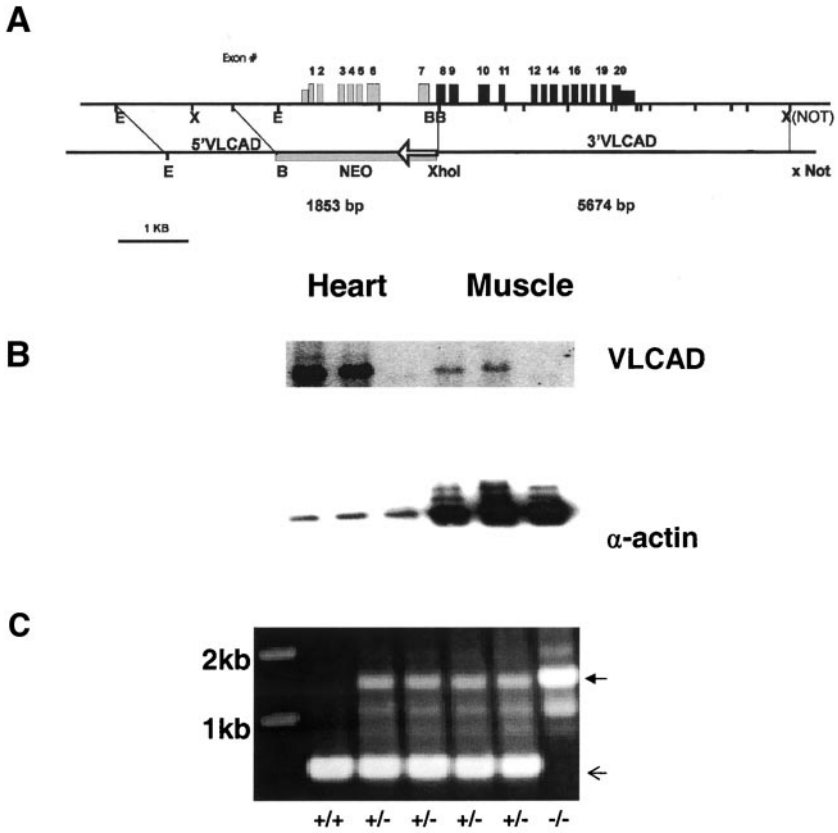

Figure 1. Strategy for targeted disruption of the VLCAD gene. A, Partial restriction enzyme map and the locations of the 20 exons are illustrated. Orientation of the neomycin cassette, as it replaces the fragment between *Bam*HI and an *Xho*I (exons 1 to 7) sites, is shown. B, Northern blot analysis of heart and skeletal muscle probed with VLCAD cDNA. Total absence of VLCAD mRNA in the VLCAD$^{-/-}$ mice is observed. C, PCR genotyping of the VLCAD-deficient mice. PCR products are 800 base pairs (bp) for the endogenous allele (open arrow), and 1500 bp for the rearranged allele (filled arrow). Genotype assignments are listed below each lane.

molecular mechanisms by which mitochondrial FAO defects cause cardiac lipidosis and cardiomyopathy are unclear. In patients dying with the fulminant form of VLCAD deficiency, postmortem examination often demonstrate lipidosis of the heart, skeletal muscle, and liver.[4–6] It has been hypothesized that the observed myocardial changes may be due to the accumulation of toxic metabolites during starvation, because fatty acid oxidation is reversibly increased during fasting stress. Consequently, it has been proposed that lethal consequences of the disease may be avoided if stress-induced hypoglycemia is prevented.[7,13]

In a murine model of VLCAD deficiency, we assessed the onset and sequence of molecular and physiological changes in the heart. The expression profile of the known fatty acid transporters was compared with the onset of histological, contractile, and electrical changes. Our findings support the hypothesis that, even in the absence of physiological stress, there are biochemical changes that predispose to cardiac lipidosis and arrhythmic death.

Materials and Methods

Gene Targeting and Generation of the VLCAD$^{-/-}$ Mice

The entire mouse VLCAD gene (5341 bp) was isolated from a murine ES-129 embryonic stem-cell genomic library. A replacement vector was designed using neomycin phosphotransferase as the positive selection marker. The recombinant allele generated by this vector disrupted the coding sequence, replacing the first 200 bp of the 5′-flanking domain, the transcription start site, and exons 1 through 7 (Figure 1A) with 1853 bp of the neomycin resistance cassette. Embryonic stem (ES) cell culture and embryo manipulation were performed using standard techniques,[14–16] with confirmatory Southern blotting of DNA from clones surviving G418 selection. ES cells from positive clones were injected into blastocysts derived from C57BL/6J mice. F1 heterozygous mice were mated to produce the three C57BL/6+129svJ VLCAD genotypes (+/+, +/−, −/−), and these experiments were performed on 2nd to 3rd generation intercrosses. Homozygous animals were shown to lack both VLCAD mRNA and protein (Figures 1B and 5A). The VLCAD-deficient mice were fed Purina rodent diet No. 5053 containing fat assayed by ether extract of 4.5% or by acid hydrolysis as 5.4%. Mice were maintained on a fixed 12-hour light/12-hour dark cycle. All protocols were approved by the Institutional Animal Care and Use Committee.

For this study, heterozygous breeding pairs were used to generate littermates representing three VLCAD genotypes (VLCAD$^{+/+}$, VLCAD$^{+/-}$, VLCAD$^{-/-}$). DNA was isolated from clipped tails using a modified salt and alcohol precipitation method (PUREGENE, Gentra). Genotyping was performed using PCR on genomic DNA, producing a 1500-bp product from the VLCAD disrupted allele, and a 800-bp band from the wild-type allele (Figure 1C), using the primer pairs ACAAGCGAGAGCCTGGACTAG and GCCAAGTTCTAATTCCATCAGAAGCTG for the rearranged gene, and TTGGAGATGCAGTCGGCTCG and TGGGTATGGGAACAACTGATC for the wild-type allele.

Histology and Electron Microscopy

Male mice representing the three possible VLCAD genotypes (VLCAD$^{-/-}$, n=8; VLCAD$^{+/-}$, n=4; VLCAD$^{+/+}$, n=4) were euthanized at two months of age. Heart weights were recorded. Further analysis was restricted to tissue isolated from the left ventricular (LV) free wall. Soleus muscle was also dissected for electron microscopy. Light microscopic histological analysis was performed on tissues fixed in 10% formalin, with 5-μm paraffin-embedded sections processed for hematoxylin and eosin staining or 5-μm frozen sections for oil red O staining. Ultrathin sections fixed overnight in glutaraldehyde, postfixed in osmium tetroxide, and embedded in epoxy resin were examined by transmission electron

microscopy (EM). Similar procedures were followed for hearts from newborn mice ($VLCAD^{-/-}$, n=2; $VLCAD^{+/-}$, n=6; $VLCAD^{+/+}$, n=2) but analysis was restricted to EM sections of the entire heart. Quantification of mitochondrial number and area was performed on digitized sections using NIH Image software (developed at the US National Institutes of Health and available on the Internet at http://rsb.info.nih.gov/nih-image).

Protein Isolation and Immunoblotting

Hearts were harvested from newborn and two month old mice representing each of the VLCAD genotypes (+/+, +/−, −/−), dissected free of atrial and pericardial tissue, and snap frozen in liquid nitrogen. Tissues were homogenized in cold 0.5%RIPA solution (PBS, 1%NP40, 0.1% SDS), with proteinase inhibitors PMSF (100 μg/mL) and Aprotinin (30 μL/mL) (Sigma). The lysate was centrifuged, and the supernatant collected. Protein concentration was determined using the Bradford method, with 20 μg of total protein per lane resolved on a 4% to 20% gradient SDS-PAGE (Ready Gels, Bio-Rad/Hercules) and then transferred to a nitrocellulose membrane. Expression of VLCAD, activator protein 2 (AP2), ACS1, adipophilin, and cytochrome *c* was assessed by Western blot using the following rabbit polyclonal antibodies: VLCAD: (Strauss laboratory, rabbit polyclonal antibody, Vanderbilt University, Nashville, Tenn); AP2 (Santa Cruz Biochemicals), cytochrome *c* (Santa Cruz Biochemicals), and ACS1[17] (kindly provided by Dr Jean Schaffer, Washington University, St Louis, Mo); monoclonal antibody against adipophilin was from Research Diagnostics. All primary antibodies were used at a dilution of 1:1000 with Luminol-based detection using horseradish peroxidase (HRP) conjugated anti-rabbit or anti-mouse IgG, and Western blot chemiluminescence reagent ECL (Amersham Pharmacia Biotech). All results presented are characteristic of at least three independent experiments.

RNA Extraction and Northern Blot

RNA was extracted from hearts using RNAeasy Midi columns (Qiagen, Co), with 10 μg of RNA per sample lane resolved on a formaldehyde-agarose gel and then transferred to a nitrocellulose membrane. Random-primes probes, labeled with [−32P]dCTP, were generated from 1 kb of the amino terminus coding sequence of the VLCAD cDNA or 1 kb of the 5′ end of peroxisome proliferator activated receptor γ coactivator-1 (PGC-1) mouse cDNA (GenBank No. NM_008904) using the Prime-It II kit (Stratagene). Hybridization was performed with QuickHyb hybridization solution at 65°C for 1 hour (Stratagene), followed by two 15 minutes washes of 2× SSC and 0.1% (wt/vol) SDS at 25°C, and two 15 minutes washes of 0.1× SSC and 0.1% SDS at 63°C. The membrane was wrapped in plastic and placed on Kodak X-OMAT AR film at −80°C. The film was exposed overnight. The membrane was stripped for reuse with 0.1× SSC buffer and 0.1% (wt/vol) SDS wash boiling solution twice for 15 minutes and reprobed with mouse β-actin as a control.

Mouse Echocardiography

Transthoracic echocardiograms were performed in 27 conscious mice (7 $VLCAD^{+/+}$, 12 $VLCAD^{+/-}$, and 8 $VLCAD^{-/-}$) at ≈2 months of age using a 15-MHz transducer (Sonos 5500 system, Agilent). Before initiation of the study, the mice were acclimated to the echo probe on two separate occasions over 1 to 2 days. Training included holding the mice in the position required for echocardiographic imaging for at least 3 minutes and conditioning the mice to probe and gel chest contact. For imaging, the mice were gently immobilized in the prone position by holding the back of the neck and the tail. Standard echocardiographic short- and long-axis views were obtained; left ventricular function, ventricular size, and wall thickness measured from M-mode frames. After intraperitoneal administration of isoproterenol at a dose of 20 ng/g, echocardiographic measurements were repeated. Digital images were obtained and analyzed offline.

Programmed Electrical Stimulation

Procedures for provocative electrical stimulation to assess arrhythmia susceptibility in mice were analogous to human measures of ventricular vulnerability.[18,19] Briefly, 20 $VLCAD^{+/+}$ and 23 $VLCAD^{-/-}$ mice, representing littermates of different genotypes aged 2.5 months to approximately 1 year, were anesthetized intraperitoneally with a ketamine/xylazine mixture, secured in the supine position, and instrumented with a mechanical tail plethysmograph (RTBP 2000, Kent Scientific). Mice were euthanized at the completion of the experiment. A lead I ECG was recorded from electrodes in the front paws. A Teflon-coated stainless steel pacing electrode (180 μm diameter) with a sharp hook bent into the tip was inserted into a 25G×5/8“ needle attached to a syringe filled with 0.5 mL of saline. The wire extended through the needle, just entering the barrel of the syringe. The electrode/needle was then advanced into the heart until blood was aspirated through the needle, ensuring proper intracardiac electrode placement. The needle was then withdrawn, leaving the pacing electrode in the heart. The return electrode for stimulation was the right front foot. A burst pacing protocol was used with 2-ms pacing pulses at 50 Hz for 50, 100, 200, and 400 beats at each of six voltages (2, 5, 7, 10, 12, and 15 V). An arrhythmia was defined as a marked change in pulse, heart rate, and ECG morphology. The duration of the arrhythmia was defined as the time from the end of the stimulus to the end of the arrhythmia.

Statistical Analysis

Statistical comparisons reflect 2-tailed *t* tests or ANOVA with correction for multiple comparisons and were performed using the Statview software package (SAS Institute Inc). Unless otherwise noted, data are expressed as mean±SD. Significance was set at $P<0.05$.

Results

Histology and Ventricular Size and Function

VLCAD mice of all genotypes were viable and fertile. Under standard laboratory conditions and diet, no differences in long-term survival were apparent. Weight did not differ by genotype at 2 months of age (Table), and no differences were apparent in growth curves or behavior to that age. There was total absence of VLCAD mRNA in heart and skeletal muscle (Figure 1B). No differences were present in the gross appearance and the heart weights of the VLCAD mice segregated by genotype (+/+, +/−, −/−) at 2 months of age (Table). Similarly, systolic and diastolic echocardiographic measurements of LV chamber and wall dimensions, fractional shortening, and heart rate did not differ significantly among mice of the three VLCAD genotypes (Table). With isoproterenol administration, FS% and HR increased in all three VLCAD genotypes, with no differences among the animals of the different genotypes (Table).

Despite normal ventricular size and function, histological assessment of the myocardium in the two month-old $VLCAD^{-/-}$ mice revealed increased numbers of degenerative fibers, collagen deposition, and vacuolated myocytes as compared with wild-type controls or heterozygotes (data not shown). Oil red O staining of frozen sections of heart muscle showed increased fat deposition in cardiac myocytes in $VLCAD^{-/-}$ mice compared with wild-type controls or heterozygotes (Figure 2). Electron microscopy of hearts from the two month-old $VLCAD^{-/-}$ animals also revealed increased numbers of mitochondria and increased lipid accumulation (ie, fatty droplets) in the cardiomyocytes compared with wild-type littermates (Figures 3A and 3B). Quantification of

Demographic and Echocardiographic Indices

Variable	Genotype			P
	VLCAD$^{-/-}$	VLCAD$^{+/-}$	VLCAD$^{+/+}$	
n	8	12	7	
Weight, g	25±4.1	28±2.1	27±4.6	NS
Heart weight, mg/g	5.2±1	5.1±0.7	4.8±0.8	NS
HR, bpm	727±160	691±71	724±68	NS
IVSd, cm	0.9±0.11	0.93±0.09	0.91±0.11	NS
LVIDd, cm	3.4±0.46	3.3±0.37	3.2±0.38	NS
LVPWd, cm	0.86±0.19	0.76±0.13	0.84±0.08	NS
IVSs, cm	1.7±0.31	1.7±0.15	1.7±0.22	NS
LVIDs, cm	1.6±0.67	1.5±0.38	1.4±0.29	NS
LVPSw, cm	1.3±0.23	1.1±0.2	1.23±0.09	NS
FS%, %	51±13	52±10	53±5	NS
HR-isuprel, bpm	723±47	702±15	748±43	NS
FS%-isuprel, %	63±6	64±6	66±5	NS

Data are mean±SD derived from gender-matched littermates. Isoproterenol response is 10 minutes after intraperitoneal injection.

IVSd indicates interventricular septal thickness in diastole; LVIDd, LV end-diastolic dimension; LVPWd, LV posterior wall thickness in diastole; IVSs, interventricular septal thickness in systole; LVIDs, LV end-systolic dimension; LVPWs, LV posterior wall thickness in systole; % FS, fractional shortening; and HR, heart rate in beats per minute (bpm).

mitochondrial area on randomly selected sections showed a statistically significant increase in mitochondrial cross sectional area (65±7% versus 41±5%, −/− versus +/+; $P<0.003$). Colocalization of mitochondria with fat droplets was often observed in the VLCAD$^{-/-}$ cardiomyocytes (arrowheads, Figure 3C). Although most VLCAD$^{-/-}$ cardiac myocyte mitochondria appeared normal, scattered bizarre and giant mitochondria were obvious in both intact and degenerative cardiac muscle cells (Figure 3C). These ultrastructural findings were not observed in cardiomyocytes from two month old wild-type or heterozygote littermates.

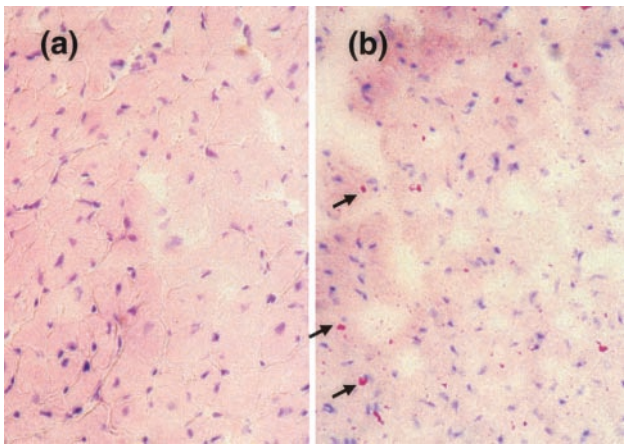

Figure 2. Oil Red O staining of heart tissue. Hematoxylin and eosin counterstain of representative 5-μm frozen sections from the left ventricular free wall. a, VLCAD$^{+/+}$. b, VLCAD$^{-/-}$. Numerous intracellular lipid vacuoles (arrows target some representative vacuoles to demonstrate appearance), not present in cardiomyocytes from wild-type mice, are noted.

Histological examination of soleus, a slow skeletal muscle with a high rate of fatty acid oxidation, from VLCAD$^{-/-}$ mice also showed marked mitochondrial proliferation, particularly in the subsarcolemmal area (Figure 3E). Irregularly sized and chaotically palisaded mitochondria in the VLCAD$^{-/-}$ skeletal myocytes contrasted with the smaller, neatly distributed single row typically present in the corresponding wild-type slow-muscle cells (Figure 3D).

In contrast to the histological findings in the two month old VLCAD-deficient mouse, no difference was observed in light or electron microscopic myocardial histology in sections from newborn hearts of the three VLCAD genotypes (data not shown). Specifically, mitochondrial morphology and number were comparable in the newborn cardiomyocytes, and there was no evidence of visible lipid deposition.

Inducibility of Ventricular Arrhythmias

Programmed stimulation was used to assess arrhythmia susceptibility in littermates of differing VLCAD genotype exceeding 2 months in age. Ventricular stimulation induced polymorphic ventricular tachycardia in 8 of 23 VLCAD-deficient mice and 0 of 20 wild-type littermate controls ($P<0.01$). Polymorphic ventricular tachycardia was identified on the basis of surface QRS complexes with beat-to-beat polymorphism differing from that observed in sinus rhythm with short R-R intervals and was associated with absence of a plethysmographic signal (Figure 4). The duration of the polymorphic ventricular tachycardia ranged from 700 to 7500 ms at rates of 510 to 714 beats per minute, compared with the sinus rates of ≈300 bpm in these anesthetized mice.

Molecular Differences in the VLCAD-Deficient Heart in the Immediate Postnatal Period

The dramatic histological abnormalities in VLCAD$^{-/-}$ hearts developed between birth and 2 months of age. We therefore determined whether biochemical abnormalities predated these anatomic changes. Protein levels of known molecular elements associated with fatty acid metabolism were assayed in newborn hearts from VLCAD$^{-/-}$ mice and their wild-type and heterozygous littermates. As expected, VLCAD protein was not detected in the hearts of newborn VLCAD$^{-/-}$ mice, but was readily detected in hearts from wide-type and heterozygous littermates (Figure 5A, row 1). AP2 is a transcription factor known to regulate VLCAD gene expression.[20] The expression of AP2 was moderately increased in the hearts of newborn VLCAD$^{-/-}$ mice as compared with wild-type controls (Figure 5A, row 2, 1.9±0.2-fold compared with control; $P<0.01$). Acyl-CoA synthase (ACS1) catalyzes the esterification of long-chain fatty acids with CoA, the first step in fatty acid oxidation, and is highly expressed in the heart. Long-chain fatty acyl-CoA synthase has been shown to play a role in long-chain fatty acid import into bacteria and a role in mammalian cell long-chain fatty acid import.[17] Protein expression of ACS1 was also increased in newborn VLCAD$^{-/-}$ hearts as compared with littermate controls (Figure 5A, row 3, 2.6±1.0-fold compared with control, $P<0.05$). Adipophilin is a marker of lipid accumulation in different tissues.[21–23] VLCAD$^{-/-}$ mice had substantially increased levels of adipophilin in the heart in the

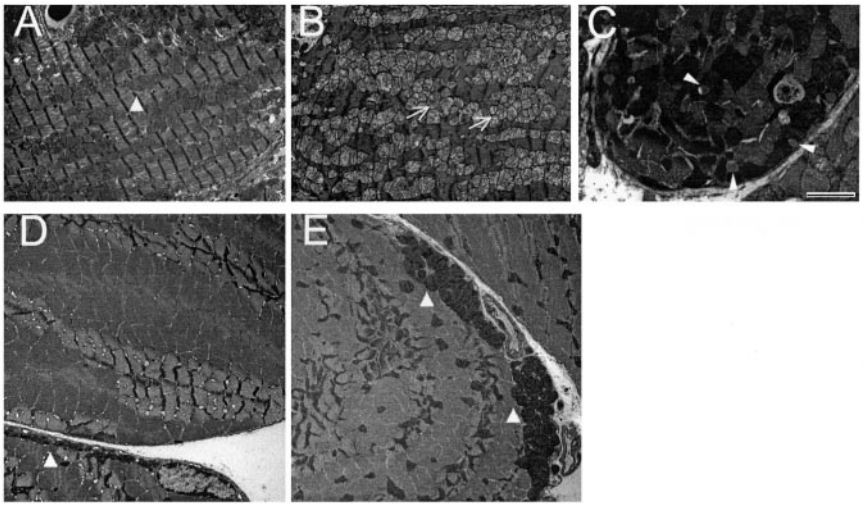

Figure 3. Electron microscopy of heart and soleus skeletal muscle. A through C, Heart: representative transmission electron micrographs of glutaraldehyde/osmium-fixed ultrathin longitudinal sections from the left ventricular free wall are shown. A, VLCAD$^{+/+}$: well-organized and uniformly distributed and sized mitochondria (arrowheads) fill a minority of the sarcoplasmic volume. B, VLCAD$^{-/-}$: mitochondria (arrows) are larger, more variable in size and morphology, and fill a substantially larger portion of the sarcoplasmic volume. In panels A and B, the cytoplasmic component can be distinguished most easily by the presence of Z bands; the relative density of cytoplasm and mitochondria is a function of EM technique. C, VLCAD$^{-/-}$, detail: subsarcoplasmic membrane fat droplets (arrowheads) are adjacent to numerous bizarre mitochondria (nearly black in this region). Bar in panel C=2 μm; magnification in panels A and B is half that of panel C. D and E, soleus. D, VLCAD$^{+/+}$: mitochondria (triangles) are uniformly sized and neatly arrayed in near-single file in the subsarcoplasmic region. E, VLCAD$^{-/-}$: mitochondria are increased in number, more heterogeneous in size, and present in disorganized aggregates in the subsarcolemmal region.

newborn period (Figure 5B, row 2, 9.6±0.6-fold compared with control; $P<0.001$). Expression of cytochrome *c* was increased in the hearts of the 1-day-old VLCAD$^{-/-}$ mice compared with VLCAD$^{+/+}$ control (Figure 5B, row 3, 3.6±0.06-fold compared with control; $P<0.001$). Expression of these factors in VLCAD heterozygotes was intermediate to that in wild-type and homozygotes (Figure 5A, 2.2±0.01-fold compared with control; $P<0.001$). In contrast, in the 2-month-old hearts, there was a trend to decreased protein expression of ACS1 (Figure 5C, 14±9% of levels in the +/+ 2-month-old adult), and no significant or suggestive changes in the levels of adipophilin or AP2 by genotype.

PGC-1 is known to induce mitochondrial biogenesis in the heart and in skeletal muscle.[24] Northern blot revealed that both the homozygous and the heterozygous VLCAD-deficient mice had increased levels of PGC-1 mRNA in the heart and skeletal muscle (Figure 5D).

Discussion

Patients with VLCAD deficiency often present with arrhythmias, before or without evidence of significant myocardial dysfunction. It is clinically important, although still unclear, whether the enzymatic defect results in established cardiac abnormalities predisposing to this potentially lethal manifestation, or whether the cardiac structural changes and heart rhythm abnormalities are a direct consequence of potentially avoidable episodes of acute stress. This mouse model of VLCAD deficiency allowed us to explore the onset of myocardial disease and the molecular events associated with these heart changes in the absence of physiological stress. A major conclusion of this study is that a cardiomyopathy, characterized by abnormal myocardial histology and increased arrhythmia susceptibility in the absence of systolic dysfunction, occurs in mice with homozygous deletion of VLCAD, in the absence of exogenously imposed stress. Biochemical changes suggestive of complex alterations in lipid metabolism and lipid transport are present in the heart at birth, whereas ultrastructural abnormalities develop postnatally. This plausibly arrhythmogenic substrate is associated with a demonstrated increase in susceptibility to the induction of polymorphic ventricular arrhythmias.

Distributed biochemical abnormalities in fatty acid oxidation have been described in mice with homogenous VLCAD deficiency achieved by gene targeting, associated with both hepatic and cardiac lipid deposition.[12] Although VLCAD is a ubiquitous enzyme, the cardiovascular system plays a dominant role in the clinical manifestations of its deficiency, suggesting an essential interaction of the gene deficiency and cardiac metabolic physiology. This report is the first to present a detailed elaboration of the cardiac phenotype, and particularly the consequences on the cardiovascular physiology, of VLCAD deficiency in the mouse. The mechanisms by which abnormalities in VLCAD engender myocellular and proarrhythmic changes could include lipotoxicity, energy starvation, and altered energy metabolism. The findings in this report support multiple mechanisms: lipotoxicity because of lipid deposition and abnormal mitochondrial and cellular architecture, energy starvation manifesting in increased mitochondrial number and area, and abnormal metabolic regulation because of the biochemical changes coincident with birth.

The biochemical changes observed may yield insights into the process of myocyte lipid accumulation. Adipophilin is a 50 kDa protein, initially cloned from mouse adipocyte cDNA library,[25] and is a marker of lipid accumulation in different tissues and a marker of lipid loading in human blood monocytes.[21–23] It has been reported to facilitate the uptake of free fatty acids in transfected Cos-7 cells.[21] However, its in vivo role in the etiology of abnormal tissue lipid accumulation is uncertain. Our finding that adipophilin expression was increased in the hearts of VLCAD$^{-/-}$ mice at birth, and preceded histological lipidosis, may suggest a role in lipid transport that needs further investigation. Further, ACS1 was markedly increased in the newborn heart, but had returned to control levels in the two month-old VLCAD-deficient heart. The ”downregulation“ of ACS1 in this setting, only apparent

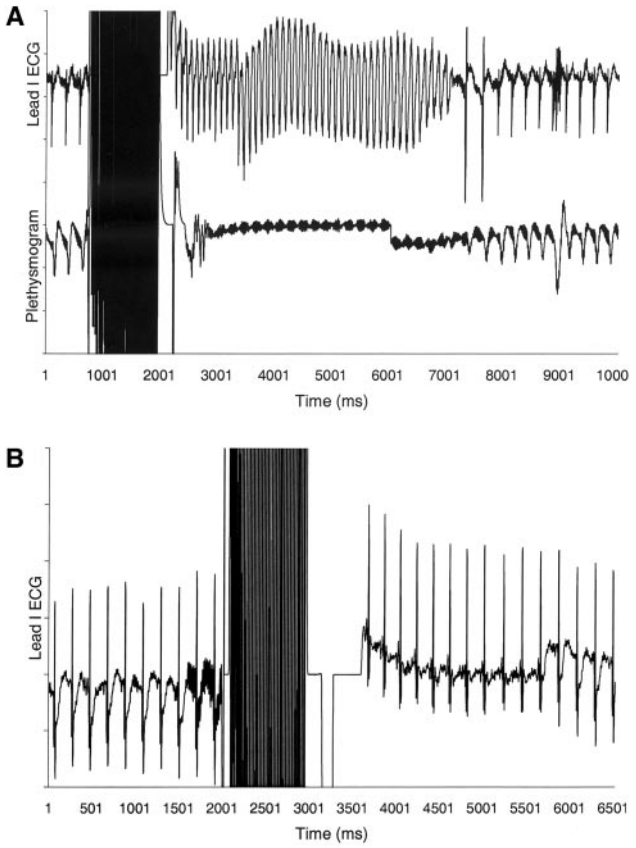

Figure 4. Induction of ventricular tachycardia (Vt). A, Continuous lead I ECG (ECG) and plethysmograph tracings are shown in VLCAD$^{-/-}$ mouse, stimulation protocol as described in the Materials and Methods section. Polymorphic ventricular tachycardia of ≈5-second duration, without significant perfusion by plethysmography, follows a 1-second induction pulse at 50 Hz. There is some saturation of the signal immediately after stimulation is terminated. B, Tracings from a VLCAD$^{+/+}$ mouse, using the same protocol. Sinus rhythm resumes after termination of the induction train (50 Hz for 1 second). Time is in milliseconds (ms) from the start of the tracing.

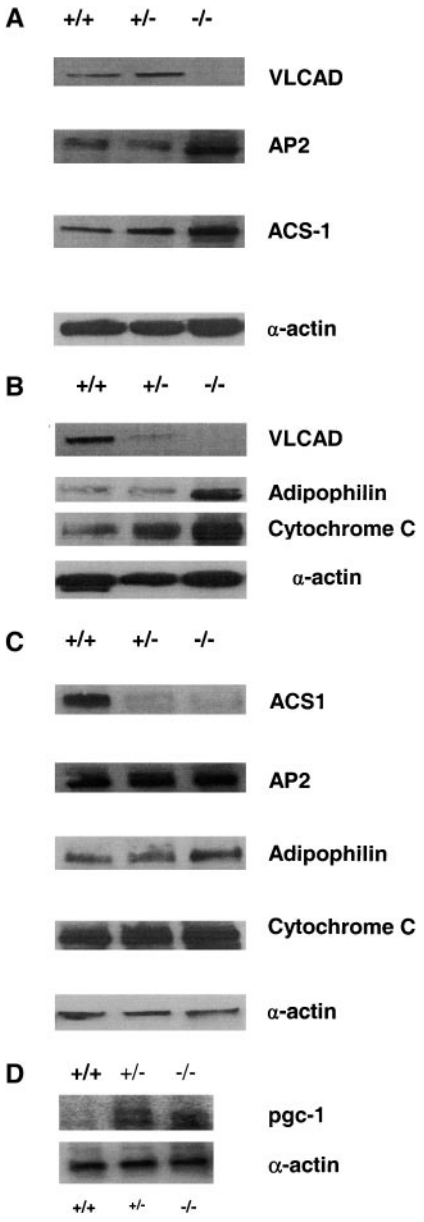

Figure 5. Patterns of gene expression in neonatal hearts. Protein and mRNA expression of genes in the newborn hearts and at 2 months of age in the three VLCAD genotypes in wild-type (+/+, VLCAD$^{+/+}$), heterozygote (+/−, VLCAD$^{+/-}$), and homozygote deleted (−/−, VLCAD$^{-/-}$). A, Western blots in newborn hearts of mice for VLCAD, AP2, and ACS1. B, Western blots in newborn hearts for adipophilin and cytochrome *c*. C, Western blots are reassessed at 2 months of age. D, Northern blot to assess mRNA expression for PGC-1 in the newborn hearts.

in comparison to the neonatal finding, would affect both the transport and esterification of long-chain fatty acids to their acyl CoA derivatives. More studies are needed to determine the molecular mechanism of acyl-CoA synthase regulation in this setting. From these data, the mechanism of lipid accumulation appears to be an imbalance between fatty acid utilization and lipid availability in the cell. The VLCAD$^{-/-}$ myocytes may represent a useful target for exploring the interrelationship of intracellular lipid transport and utilization, and the regulation of energy metabolism.

PGC-1 is a master regulator of energy homeostasis, and is induced in the heart with increased energy demand.[24] The dramatic induction in PGC-1 observed in the VLCAD-deficient newborn hearts may reflect relative energy starvation in the immediate postnatal period. In turn, PGC-1 may drive the marked increase in mitochondrial number in the VLCAD-deficient hearts.[24] Similarly, AP2 is also induced in the newborn heart. AP2 is a transcription factor known to regulate the VLCAD gene,[20] and its induction may reflect a feedback-regulated circuit involving the VLCAD gene. These changes could also be a reflection of physiological perinatal stress. However, because intrauterine cardiac energy generation is predominantly independent of lipid utilization,[4,6,7] these changes are probably not a function of prenatal myocardial energy starvation. Altogether, these changes reinforce the idea that the transcriptional changes observed in the VLCAD-deficient heart reflect an attempt to "compensate" for the lack of the enzyme when increased energy from fatty acid oxidation typically occurs.

There are several limitations of the study. Expression studies were performed at two times points, immediately after

birth and at 2 months of age, and were restricted to limited set of biochemical markers. A sequential analysis using a gene array or a proteomics approach might yield additional information about regulatory networks and their relationship to the changes in cardiac substrate preference temporally associated with weaning. A single measure of susceptibility to ventricular arrhythmias was used, whereas clinically fatty acid oxidation defects are associated with atrial, ventricular tachyarrhythmias, and other conduction abnormalities. Because strain background is known to have important effects on metabolic pathways, it will be necessary to explore the interrelation of strain and metabolic gene pathway patterns. Finally, although systolic dysfunction was not observed in the young adult mice studied here, it may develop with age or in the presence of defined metabolic stress. Additionally, this mouse model of VLCAD deficiency has a less severe phenotype than what is observed in humans with forms of the disease reflecting total absence of enzymatic activity. For example, in a study of genotype:phenotype correlation, 15 of 18 VLCAD patients had clinical evidence of cardiac involvement, with 12 of the 15 showing dilated or hypertrophic cardiomyopathy.[5] The differences between human and murine phenotype may reflect differences in diet, inevitable episodes of stress, or the quantitative but not absolute differences in substrate preference among the long- and very-long-chain fatty acids among different species.[12] Nonetheless, essential characteristics of the human disease are replicated.

Recognition of fatty acid oxidation defects, and particularly VLCAD deficiency, as a causal factor in cardiomyopathy and sudden death is relatively recent, without long-term longitudinal studies. In fact, systematic studies of patients and the natural history of the disease are difficult, because patients are often clinically asymptomatic before a catastrophic presentation. Although it is always problematic to extrapolate from murine models to human disease, the findings in the mouse suggest at least the following avenues for query in humans: whether heterozygotes, in which milder forms of the biochemical abnormalities are noted, also have a phenotypically mild form of the disease, and whether VLCAD deficiency forms an additive substrate for arrhythmia susceptibility that can interact with acquired cardiac abnormalities such as hypertension, diabetes, or infarction. Provocative tests for arrhythmia vulnerability might be informative, for example, in patients without evidence of systolic dysfunction, or in the obligate heterozygote parents of the probands.

In conclusion, directed evaluation of the cardiovascular phenotype in mice with homozygous absence of VLCAD reveals ultrastructural abnormalities including cardiomyocyte lipid deposition and mitochondrial proliferation. These cellular changes are associated with an enhanced susceptibility to the induction of ventricular arrhythmias in the presence of preserved ventricular systolic function, recapitulating important aspects of the associated human disease entity. It is notable that clinical surveys of patients with VLCAD deficiency demonstrate a clear correlation of disease genotype (that is, complete versus partial deletion) with clinical phenotype, which has often proved elusive in other fatty acid defects such as MCAD deficiency. The findings in this report, together with this clinically derived insight, suggest that mice with VLCAD deficiency may represent a tractable model system in which the pathophysiological relationships of altered fatty acid oxidation, intracellular fatty acid homeostasis, myocardial dysfunction, and arrhythmias can be explored.

Acknowledgments

This work was supported by fellowship grants from the Robert Wood Johnson Foundation and the Vanderbilt Physician-Scientist Program (V.J.E.), NIH/NHLBI (A.W.S.), and NIH/NIDDK (Mouse Metabolic Phenotyping Center; J.N.R.), and American Heart Association (Established Investigator Award to R.A.M.).

References

1. Andresen BS, Olpin S, Poorthuis BJ, Scholte HR, Vianey-Saban C, Wanders R, Ijlst L, Morris A, Pourfarzam M, Bartlett K, Baumgartner ER, deKlerk JB, Schroeder LD, Corydon TJ, Lund H, Winter V, Bross P, Bolund L, Gregersen N. Clear correlation of genotype with disease phenotype in very-long-chain acyl-CoA dehydrogenase deficiency. *Am J Hum Genet*. 1999;64:479–494.
2. Bertrand C, Largilliere C, Zabot MT, Mathieu M, Vianey-Saban C. Very long chain acyl-CoA dehydrogenase deficiency: identification of a new inborn error of mitochondrial fatty acid oxidation in fibroblasts. *Biochim Biophys Acta*. 1993;1180:327–329.
3. Hale DE, Bennett MJ. Fatty acid oxidation disorders: a new class of metabolic diseases. *J Pediatr*. 1992;121:1–11.
4. Kelly DP, Strauss AW. Inherited cardiomyopathies. *N Engl J Med*. 1994;330:913–919.
5. Mathur A, Sims HF, Gopalakrishnan D, Gibson B, Rinaldo P, Vockley J, Hug G, Strauss AW. Molecular heterogeneity in very-long-chain acyl-CoA dehydrogenase deficiency causing pediatric cardiomyopathy and sudden death. *Circulation*. 1999;99:1337–1343.
6. Roe CR, Ding J. Mitochondrial fatty acid oxidation disorders. In: Scriver CR, Beaudet AL, Sly WS, Valle D, eds. *The Metabolic and Molecular Basis of Inherited Disease*. New York, NY: McGraw-Hill; 2000: 2297–2326.
7. Strauss AW, Powell CK, Hale DE, Anderson MM, Ahuja A, Brackett JC, Sims HF. Molecular basis of human mitochondrial very-long-chain acyl-CoA dehydrogenase deficiency causing cardiomyopathy and sudden death in childhood. *Proc Natl Acad Sci U S A*. 1995;92:10496–10500.
8. Vockley J. The changing face of disorders of fatty acid oxidation. *Mayo Clin Proc*. 1994;69:249–257.
9. He G, Yang BZ, Roe DS, Teramoto R, Aleck K, Grebe TA, Roe CR, Ding JH. Identification of two novel mutations in the hypoglycemic phenotype of very long chain acyl-CoA dehydrogenase deficiency. *Biochem Biophys Res Commun*. 1999;264:483–487.
10. Aoyama T, Souri M, Ushikubo S, Kamijo T, Yamaguchi S, Kelley RI, Rhead WJ, Uetake K, Tanaka K, Hashimoto T. Purification of human very-long-chain acyl-coenzyme A dehydrogenase and characterization of its deficiency in seven patients. *J Clin Invest*. 1995;95:2465–2473.
11. Roe CR, Sweetman L, Roe DS, David F, Brunengraber H. Treatment of cardiomyopathy and rhabdomyolysis in long-chain fat oxidation disorders using an anaplerotic odd-chain triglyceride. *J Clin Invest*. 2002;110: 259–269.
12. Cox KB, Hamm DA, Millington DS, Matern D, Vockley J, Rinaldo P, Pinkert CA, Rhead WJ, Lindsey JR, Wood PA. Gestational, pathologic and biochemical differences between very long-chain acyl-CoA dehydrogenase deficiency and long-chain acyl-CoA dehydrogenase deficiency in the mouse. *Hum Mol Genet*. 2001;10:2069–2077.
13. Brown-Harrison MC, Nada MA, Sprecher H, Vianey-Saban C, Farquhar J Jr, Gilladoga AC, Roe CR. Very long chain acyl-CoA dehydrogenase deficiency: successful treatment of acute cardiomyopathy. *Biochem Mol Med*. 1996;58:59–65.
14. Matise MP, Auerbach W, Joyner AL. Production of targeted embryonic stem cell clones. In: Joyner AL, ed. *Gene Targeting: A Practical Approach*. Oxford, UK: Oxford University Press; 2000:101–132.
15. Papaioannou VE, Johnson RS. Production of chimera by blastocysts and morula injection of targeted ES cells. In: Joyner AL, ed. *Gene Targeting: A Practical Approach*. Oxford, UK: Oxford University Press; 2000: 133–175.

16. Robertson E, Bradley A, Kuehn M, Evans M. Germ-line transmission of genes introduced into cultured pluripotential cells by retroviral vector. *Nature*. 1986;323:445–448.
17. Gargiulo CE, Stuhlsatz-Krouper SM, Schaffer JE. Localization of adipocyte long-chain fatty acyl-CoA synthetase at the plasma membrane. *J Lipid Res*. 1999;40:881–892.
18. Garan H, Fallon JT, Ruskin JN. Nonsustained polymorphic ventricular tachycardia induced by electrical stimulation in 3 week old canine myocardial infarction. *Am J Cardiol*. 1981;48:280–286.
19. Kowey PR, Friehling TD, Wetstein L, O'Connor KM, Kelliher GJ. Influence of site of stimulation on measurement of ventricular vulnerability in the normal and ischemic feline heart. *Am J Cardiol*. 1984; 54:421–423.
20. Zhou Y, Kelly DP, Strauss AW, Sims H, Zhang Z. Characterization of the human very-long-chain acyl-CoA dehydrogenase gene promoter region: a role for activator protein 2. *Mol Genet Metab*. 1999;68:481–487.
21. Buechler C, Ritter M, Duong CQ, Orso E, Kapinsky M, Schmitz G. Adipophilin is a sensitive marker for lipid loading in human blood monocytes. *Biochim Biophys Acta*. 2001;1532:97–104.
22. Heid HW, Schnolzer M, Keenan TW. Adipocyte differentiation-related protein is secreted into milk as a constituent of milk lipid globule membrane. *Biochem J*. 1996;320(pt 3):1025–1030.
23. Heid HW, Moll R, Schwetlick I, Rackwitz HR, Keenan TW. Adipophilin is a specific marker of lipid accumulation in diverse cell types and diseases. *Cell Tissue Res*. 1998;294:309–321.
24. Lehman JJ, Barger PM, Kovacs A, Saffitz JE, Medeiros DM, Kelly DP. Peroxisome proliferator-activated receptor γ coactivator-1 promotes cardiac mitochondrial biogenesis. *J Clin Invest*. 2000;106: 847–856.
25. Jiang HP, Serrero G. Isolation and characterization of a full-length cDNA coding for an adipose differentiation-related protein. *Proc Natl Acad Sci U S A*. 1992;89:7856–7860.